Electronic Supplementary Material (ESI) for Journal of Materials Chemistry C.

Supporting Information

A Multi-State Fluorescent Switch with Multifunction of AIE, Methanol-Responsiveness, Photochromism and Mechanochromism

Lili Huang,[a] Yixin Qiu,[a] Chenyang Wu,[a] Zhiyong Ma,*[a] Zhihao Shen[b] *and* Xinru Jia[b]

[a] *Beijing State Key Laboratory of Organic-Inorganic Composites, College of Chemical Engineering, Beijing University of Chemical Technology, Beijing 100029, China. *E-mail: mazhy@mail.buct.edu.cn*

[b] *Beijing National Laboratory for Molecular Sciences, Key Laboratory of Polymer Chemistry and Physics of the Ministry of Education, College of Chemistry and Molecular Engineering, Peking University, Beijing 100871, China.*

1. Materials and General Methods

All the solvents and reactants were purchased from commercialized companies and used as received without further purification except for specifying otherwise.

^{1}H NMR was recorded on the 400 MHz spectrometer (Bruker ARX400) and ^{13}C NMR spectra were recorded on the Bruker 125 MHz spectrometer at room temperature with $CDCl_3$ as the solvent and tetramethylsilane (TMS) as the internal standard. ESI high resolution mass-spectra (HRMS) were acquired on a Bruker Apex IV FTMS mass spectrometer. UV-vis spectra were acquired on the Hitachi U-4100 UV-vis spectrophotometer. Steady fluorescence spectra were performed on the Hitachi F-7000 or Edinburgh Instruments FLS920 fluorescence spectrophotometer. The calculation of quantum yield was performed on the Nanolog/FluoroLog-3-2-Ihr320 combined measurement system for infrared fluorescence equipped with an integrating sphere. Fluorescence lifetime were acquired on the Lifespec-Red Picosecond Lifetime Spectrometer (λ_{ex}=365nm). Differential scanning calorimetry (DSC) measurement was carried out by using TA instruments Q100 DSC. Wide-angle X-ray diffraction (WAXD) experiments were performed on a Philips X'PertPro diffractometer with a 3 kW ceramic tube as the X-ray source (Cu Kα) and an X'celerator detector.

The ground state geometries were fully optimized by the density functional theory (DFT) method with the Becke three-parameter hybrid exchange and the Lee-Yang-Parr correlation functional (B3LYP) and 6-31G(d,p) basis set using the Gaussian 09 software package. Frequency checks were carried out after each geometry optimization to ensure that the minima on the potential energy surfaces were found.

2. Synthesis of targeted molecule

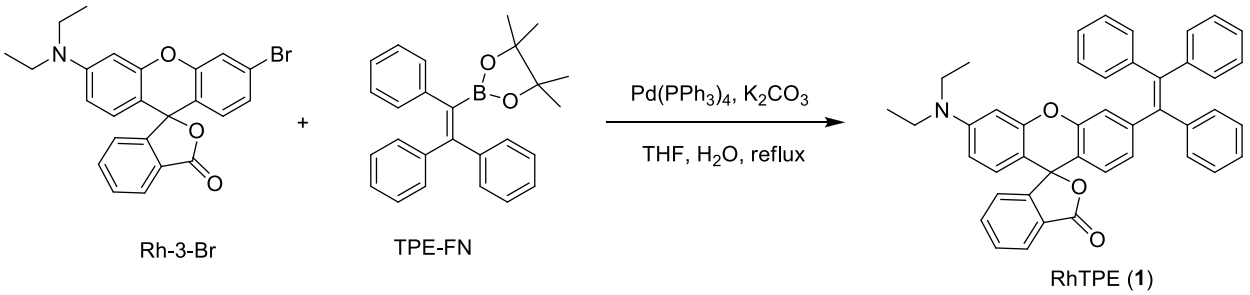

Scheme S1. The synthetic route to **RhTPE**.

RhTPE

Rh-3-Br (212 mg, 0.470 mmol), TPE-FN (195 mg, 0.51 mmol), K_2CO_3 (87.8 mg,0.64 mmol) and $Pd(PPh_3)_4$ were all placed in a 50 mL schlenk flask, and the system was purged with nitrogen for 10 min. THF (10 mL, HPLC grade) and 4 mL of degassed deionized water was then carefully added.[1] The solution was refluxed under 90℃ for 36 h and then cooled down to room temperature. The solvent in the mixture was evaporated under reduced pressure and then the crude product was purified by column chromatography with silica gel (ethyl acetate: petroleum ether=1:5 as the eluent). The pure product was gained as a white powder. Yield: 78%.

^{1}H NMR (400 MHz, $CDCl_3$) ,δ/ppm :7.96 (s, 1H, Ar-H), 7.68 – 7.53 (m, 2H, Ar-H), 7.51 – 7.21 (m, 2H, Ar-H), 7.16 (s, 1H, Ar-H), 7.08 (s, 6H, Ar-H), 7.02 (s, 5H, Ar-H), 6.97 – 6.87 (m, 2H, Ar-H), 6.83 – 6.73 (m, 1H, Ar-H), 6.70 – 6.60 (m, 1H, Ar-H), 6.51 (ddd, 2H, Ar-H), 6.43 – 6.34 (m, 1H, Ar-H), 6.32 (dt, 1H, Ar-H), 3.32 (dq, 4H, -CH_2-), 1.14 (dt, 6H, -CH_3).

^{13}C NMR ^{13}C NMR (101 MHz, $CDCl_3$) δ/ppm: 169.71, 153.45, 153.11, 153.00, 152.89, 151.41, 151.05, 149.61, 146.24, 144.30, 143.78, 143.44, 143.20, 143.11, 142.77, 142.13, 140.41, 139.96, 139.62, 137.37, 134.74, 131.32, 131.19, 131.01, 130.90, 130.06, 129.45, 129.26 128.84 , 127.97, 127.89 , 127.82, 127.69, 127.22, 127.07, 126.93, 126.82, 126.66, 126.41, 124.85, 124.52, 124.09, 123.98, 119.53, 117.41, 108.31, 105.16, 97.69, 84.19, 44.50, 12.54.

HR-ESI-MS Calcd. For $C_{44}H_{35}NO_3$ $[M+H]^+$: 626.26897. Found: 626.26852.

3. NMR spectra and HR-MS of RhTPE

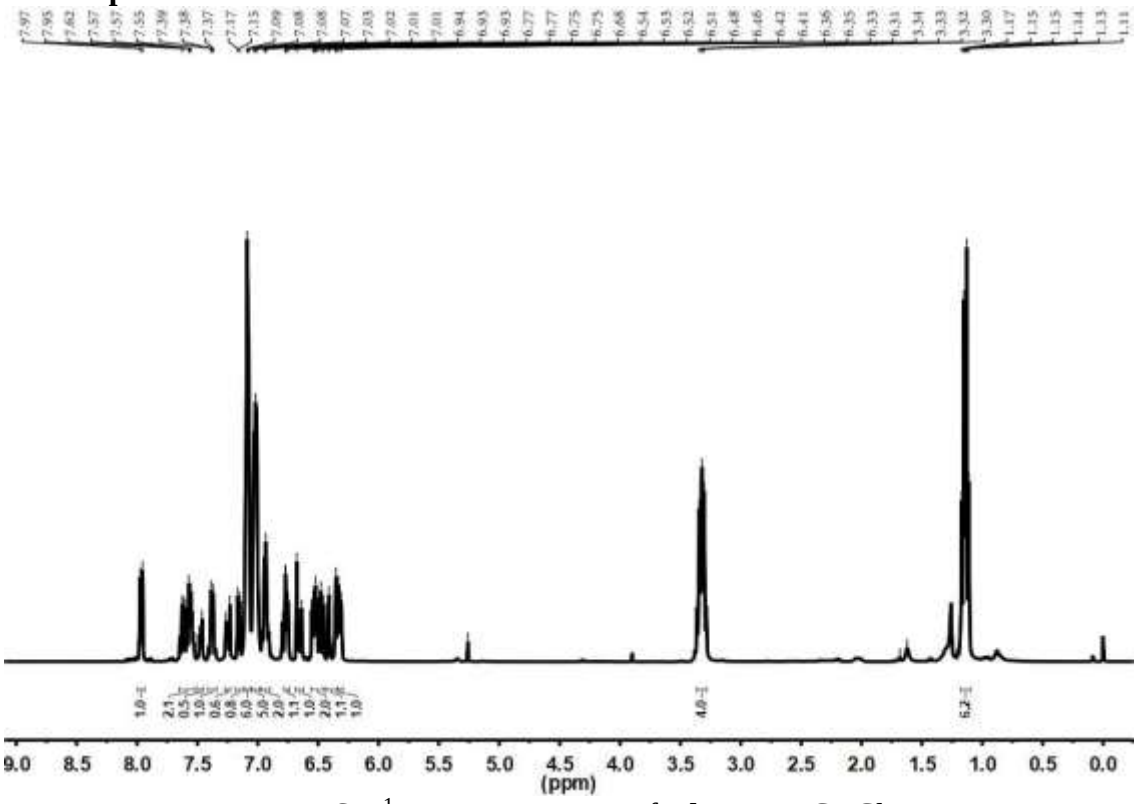

Figure S1. ^{1}H NMR spectrum of **RhTPE** in $CDCl_3$

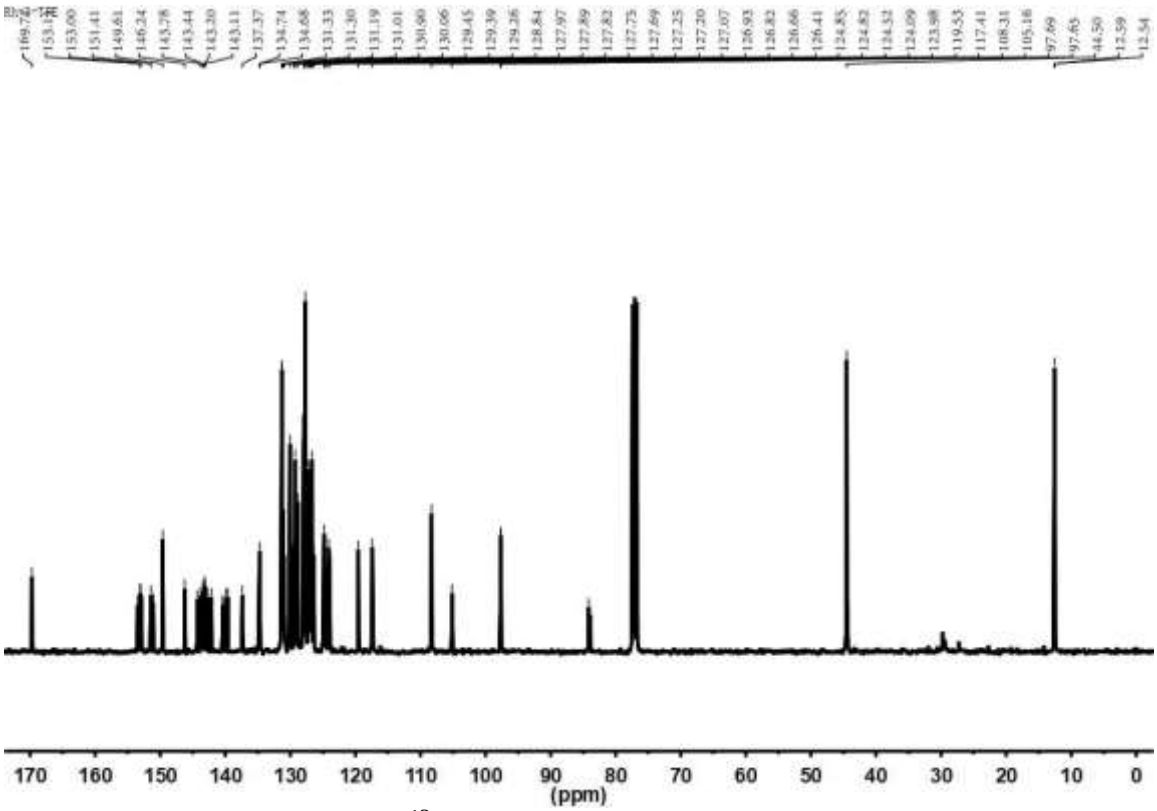

Figure S2. ^{13}C NMR spectrum of **RhTPE** in $CDCl_3$.

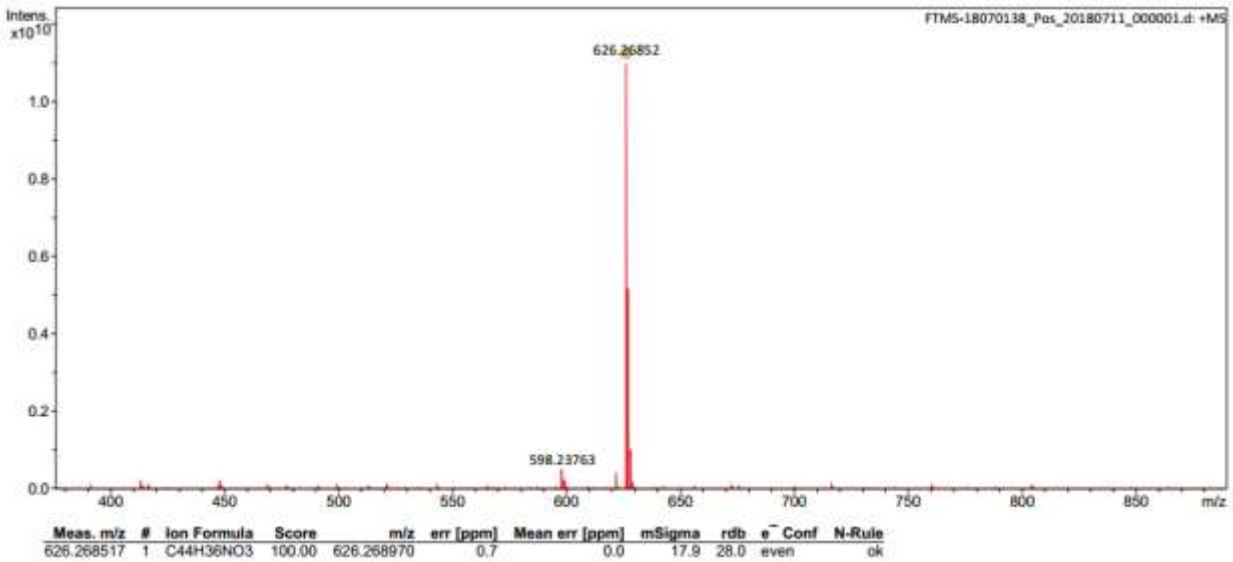

Meas. m/z	#	Ion Formula	Score	m/z	err [ppm]	Mean err [ppm]	mSigma	rdb	e⁻ Conf	N-Rule
626.268517	1	C44H36NO3	100.00	626.268970	0.7	0.0	17.9	28.0	even	ok

Figure S3. HR-MS spectrum of **RhTPE**.

4. RhTPE in DCM solution

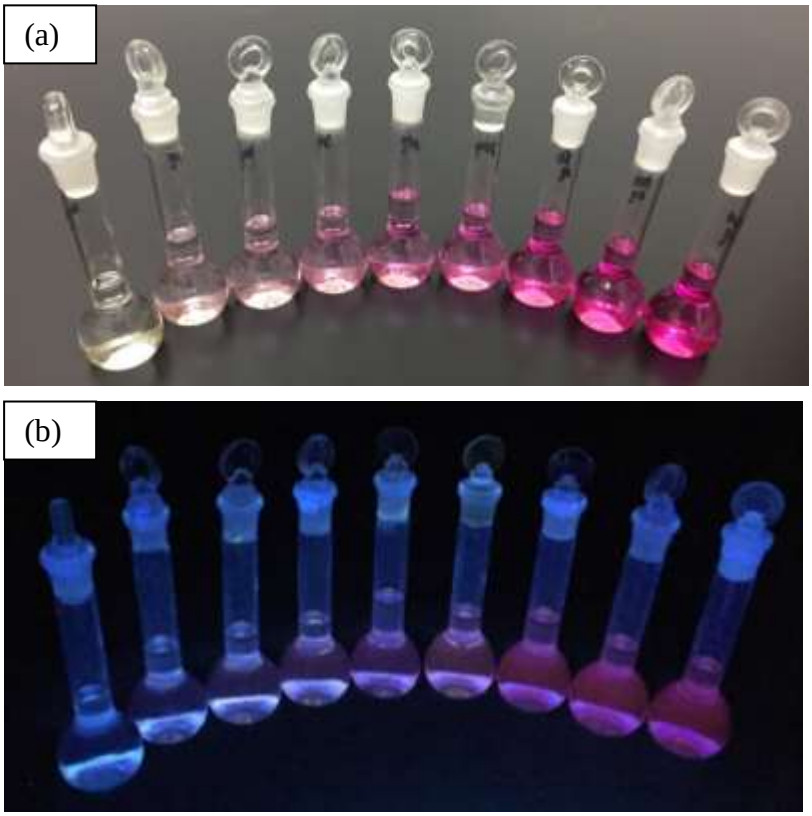

Figure S4. Optical images of RhTPE DCM solution (10 μM) with the addition of TFA (0 eq to 500 eq) under visible light (a) and UV light (b).

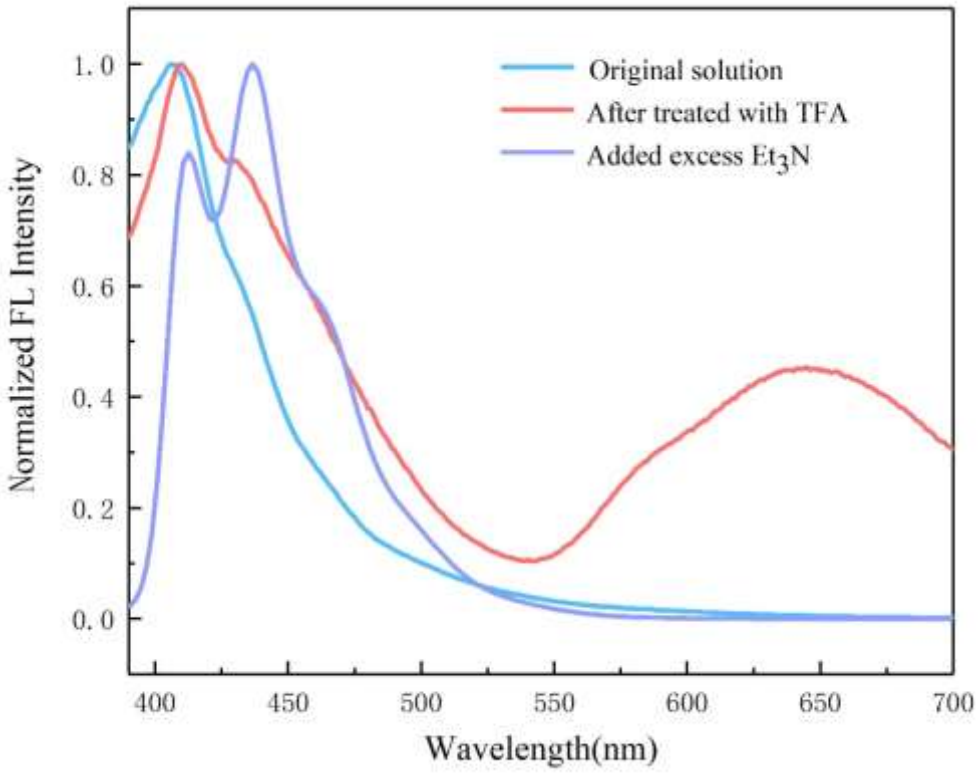

Figure S5. Fluorescence spectra of acidified **RhTPE** in DCM solution (~1×10^{-5} M) after treatment with excess Et_3N.

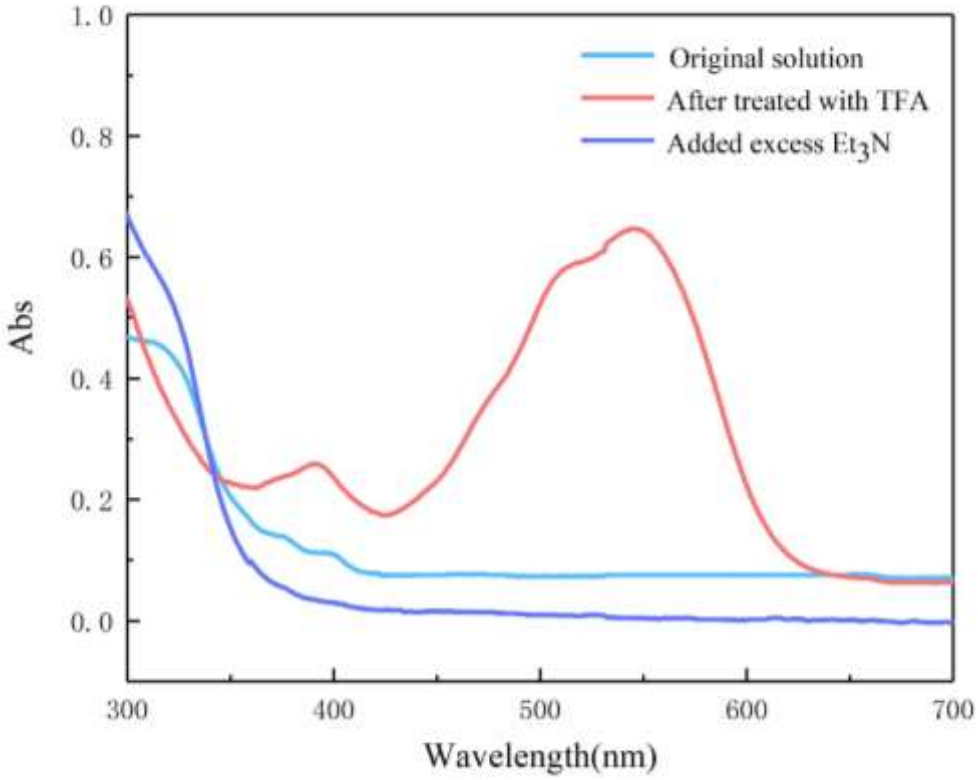

Figure S6. Absorption spectrum of acidified **RhTPE** in DCM solution (~1×10^{-5} M) after treatment with excess Et_3N.

5. Molecular simulation

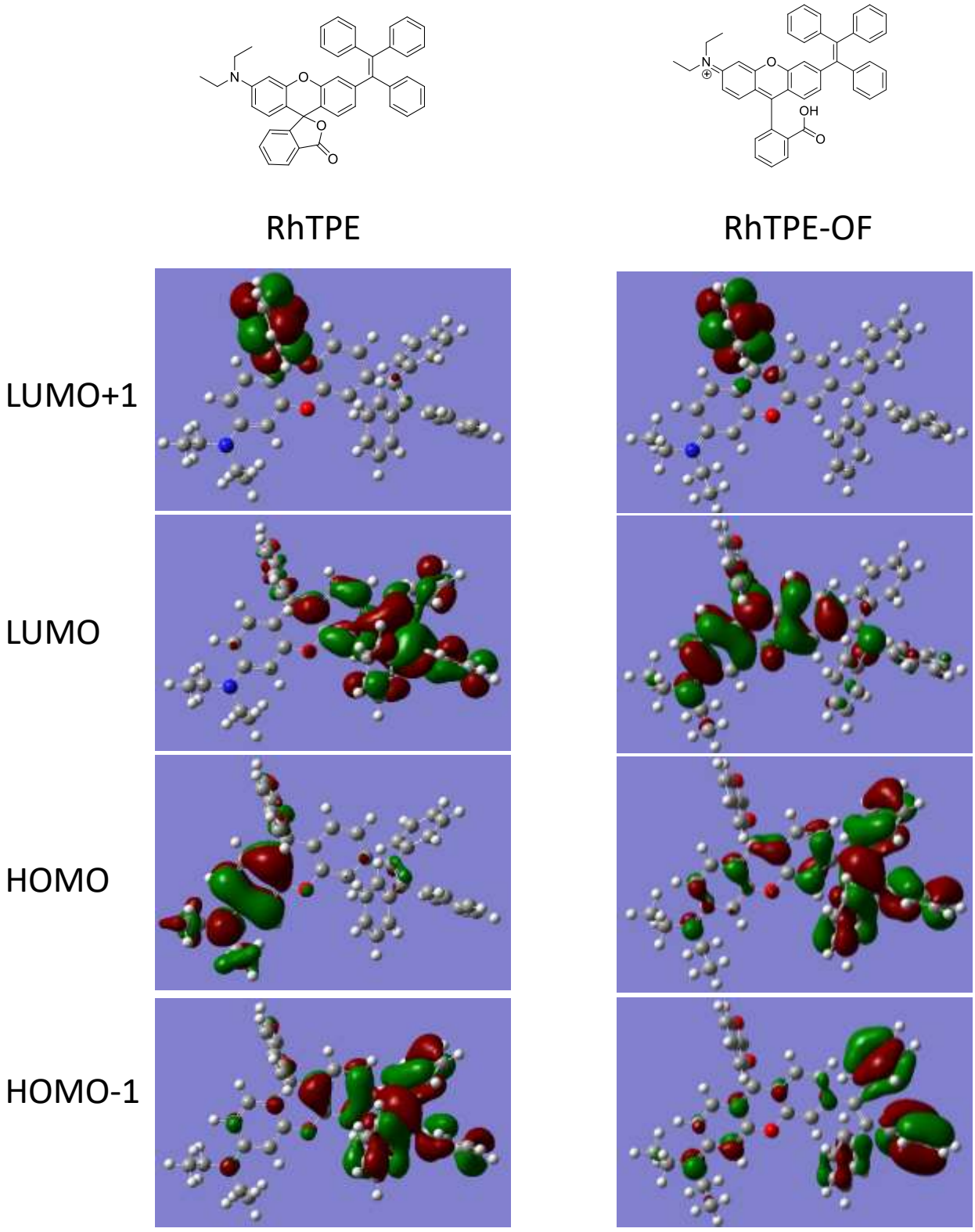

Figure S7. Calculated HOMO–LUMO orbitals of RhTPE and RhTPE-OF using the B3LYP/6-31g(d,p) basis set.[2]

6. pKa values and polarity of the twelve solvents

Table S1. pKa values and polarity (empirical parameter) of the twelve solvents at room temperature.

solvent	**pKa**	**polarity**	**polarity ET(h)[a]**
ethanol	16	4.3	0.654
methanol	**15.5**	**6.6**	**0.762**
chloroform	15.5	4.4	0.259
toluene	41	2.4	0.099
EA	25	4.3	0.228
acetone	19.3	5.4	0.355
DMSO	35	7.2	0.444
THF	-	4.2	0.207
DMF	-	6.4	0.404
MeCN	25	6.2	0.46
DCM	-	3.4	0.309
Water	15.7	10.2	1

a. CRC Handbook of Data on Organic Compounds. Vol. I and II, CRC Press, Boca Raton/Florida 1985.

7. Weak Photochromism of RhTPE in DMF

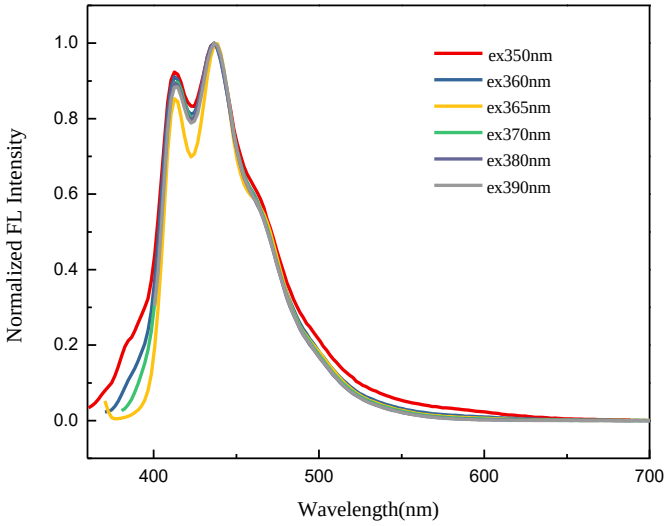

Figure S8. Fluorescence spectra of the DMF solutions (400 μM) using different excitation wavelength.

8. Fluorescence excitation spectra of RhTPE in eleven different solvent

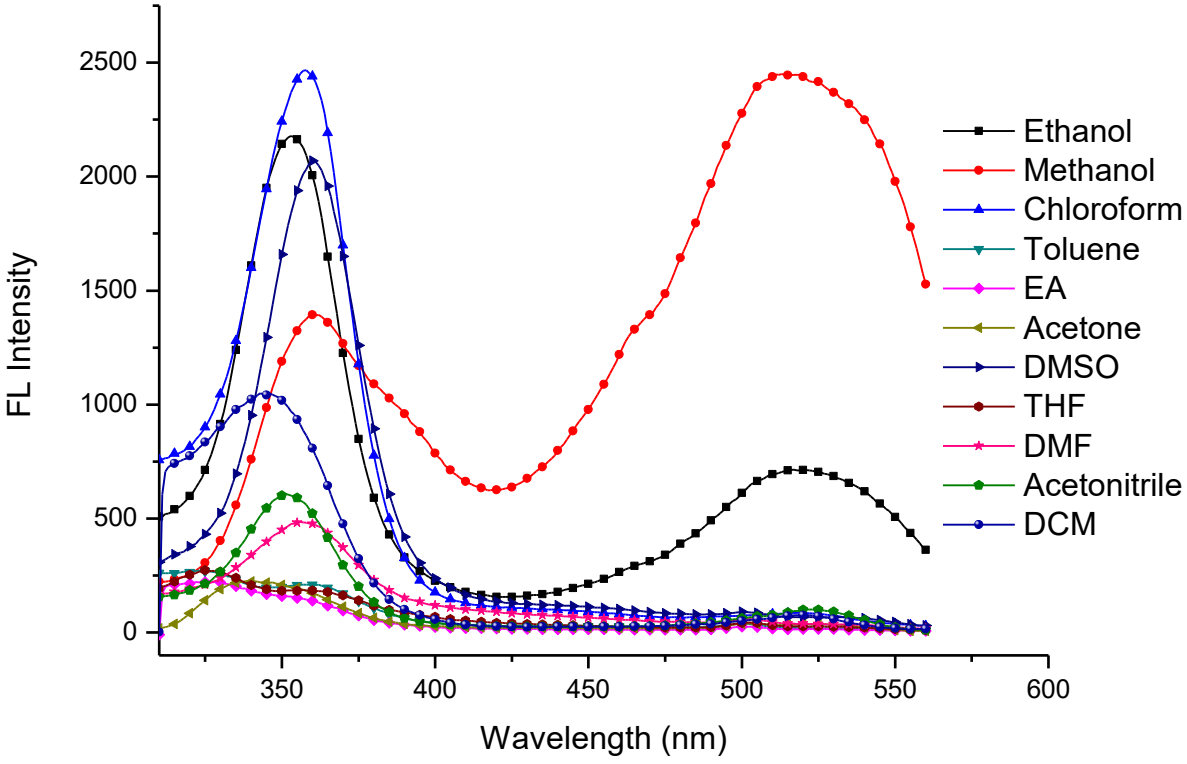

Figure S9. Fluorescence excitation spectra of RhTPE solution (400 μM, λ_{em}=590 nm) in eleven different solvents.

9. XRD profiles

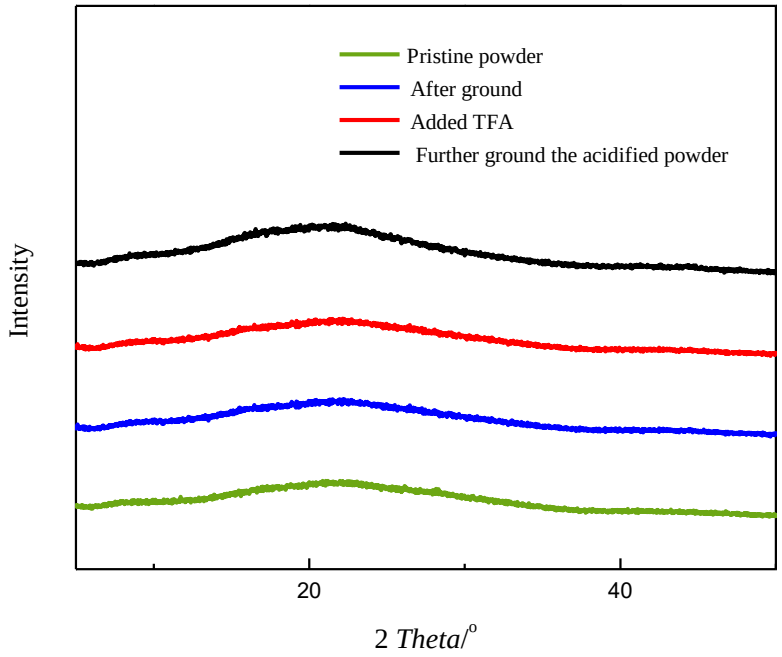

Figure S10. WAXD profiles of pristine powder of RhTPE, ground powder of RhTPE, TFA-fumed pristine RhTPE powder and TFA-fumed RhTPE powder after grinding.

10. DSC curves

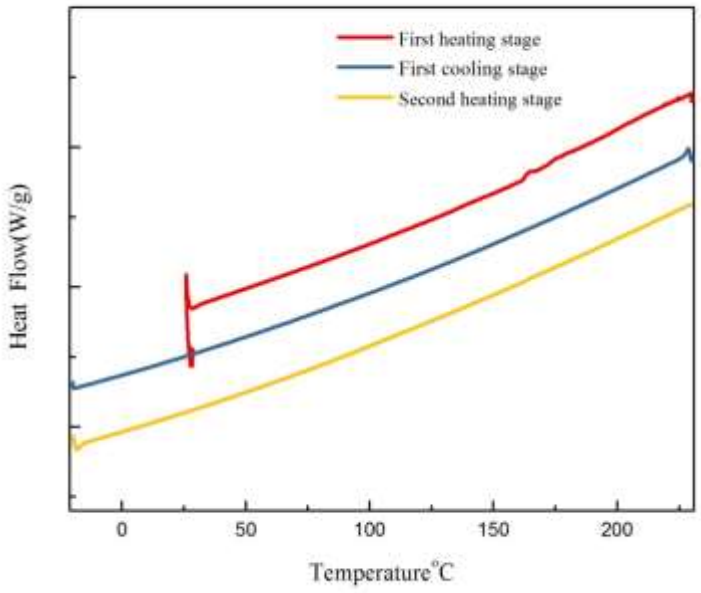

Figure S11. DSC curves of the pristine RhTPE powder.

11. Application demonstration

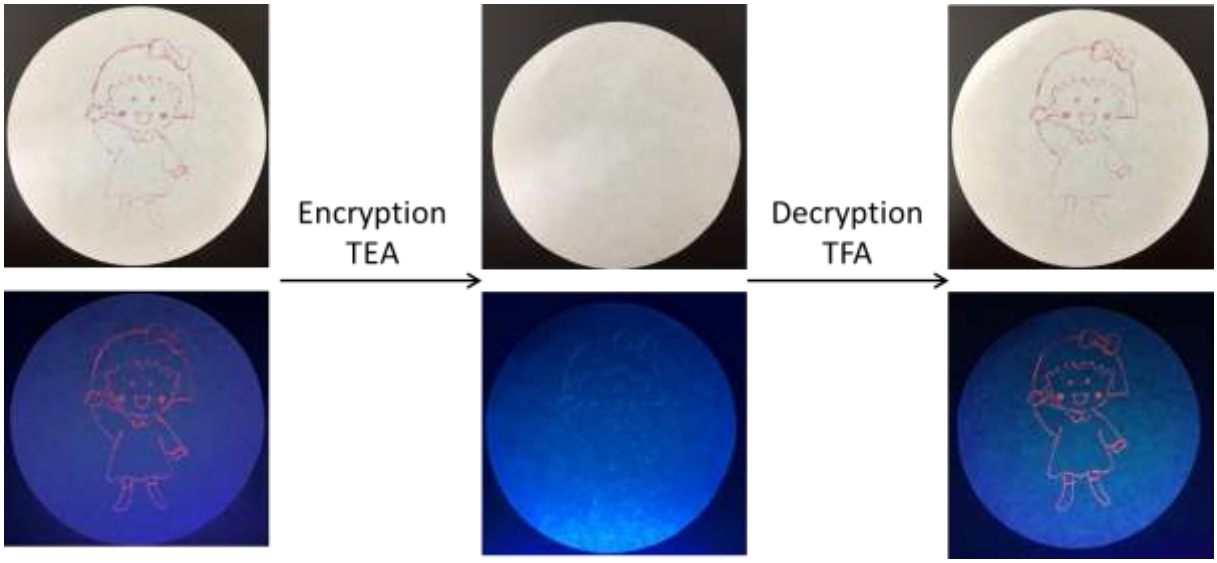

Figure S12. Information encryption and decryption by TEA and TFA.

References

[1] F. S. M. Ali, W. Zhiming, G. C. Ching, M. P. N., W. Wenbo, M. Duo, N. L. Guan, Z. Zujin, T. B. Zhong and L. Bin, *Adv. Mater.*, 2017, **29**, 1604100.

[2] Gaussian 09, Revision A.02, G. W. T. M. J. Frisch, H. B. Schlegel,G. E. Scuseria, J. R. C.M. A. Robb, G. Scalmani, V. Barone, B. Mennucci,H. N. G. A. Petersson, M. Caricato, X. Li, H. P. Hratchian,J. B. A. F. Izmaylov, G. Zheng, J. L. Sonnenberg, M. Hada, K. T. M.Ehara, R. Fukuda, J. Hasegawa, M. Ishida, T. Nakajima, O. K. Y.Honda, H. Nakai, T. Vreven, J. A. Montgomery Jr., F. O. J. E. Peralta,M. Bearpark, J. J. Heyd, E. Brothers, V. N. S. K. N. Kudin, R. Kobayashi,J. Normand, A. R. K. Raghavachari, J. C. Burant, S. S. Iyengar,J. Tomasi, N. R. M. Cossi, J. M. Millam, M. Klene, J. E. Knox,J. B. Cross, C. A. V. Bakken, J. Jaramillo, R. Gomperts, R. E. Stratmann,A. J. A. O. Yazyev, R. Cammi, C. Pomelli, J. W. Ochterski,K. M. R. L. Martin, V. G. Zakrzewski, G. A. Voth, J. J. D. P. Salvador,S. Dapprich, A. D. Daniels, J. B. F. O. Farkas, J. V. Ortiz, J. Cioslowski,D. J. Fox, Gaussian, Inc., Wallingford CT, 2009.